



HHS PUBLIC ACCESS

Author manuscript

Bioorg Med Chem Lett. Author manuscript; available in PMC 2015 September 14.

Published in final edited form as:

Bioorg Med Chem Lett. 2014 February 1; 24(3): 963–968. doi:10.1016/j.bmcl.2013.12.061.

Constrained TRPV1 agonists synthesized via silver-mediated intramolecular azo-methine ylide cycloaddition of α -iminoamides

Thomas O. Painter^a, Krisztian Kaszas^b, Jacklyn Gross^b, Justin T. Douglas^c, Victor W. Day^c, Michael J. Iadarola^b, and Conrad Santini^{a,†,*}

^aCenter for Chemical Methodologies and Library Development, The University of Kansas, 2034 Becker Drive, Lawrence, KS 66047, United States

^bDepartment of Perioperative Medicine, Clinical Center, National Institutes of Health, Building 10, Room 2C401, 10 Center Drive, MSC 1510, Bethesda, MD 20892-1510, United States

^cThe University of Kansas Molecular Structures Group, 1251 Wescoe Hall Drive, Lawrence, KS 66045, United States

Abstract

As part of an effort to identify agonists of TRPV1, a peripheral sensory nerve ion channel, high throughput screening of the NIH Small Molecule Repository (SMR) collection identified MLS002174161, a pentacyclic benzodiazepine. A synthesis effort was initiated that ultimately afforded racemic *seco* analogs **12** of the SMR compound via a silver mediated intramolecular [3+2] cycloaddition of an azo-methine ylide generated from α -iminoamides **11**. The cycloaddition set four contiguous stereocenters and, in some cases, also spontaneously afforded imides **13** from **12**. The synthesis of compounds **12**, the features that facilitated the conversion of **12**–**13**, and their partial agonist activity against TRPV1 are discussed.

Keywords

Chronic pain; Peripheral nerve ion channels; Intramolecular cycloaddition; TRPV1 agonists

One of the most problematic areas in contemporary clinical practice is the long-term management of chronic pain. There are numerous analgesics available for this purpose, many of which act at the opioid receptors in the CNS.¹ While these drugs are safe and effective if administered under rigorously controlled conditions, long-term use of opiates inevitably leads to tolerance, physical dependence and sometimes depression.¹ More troublesome, however, is that the mood altering effects of opiates are such that, under real life conditions, these medications are often diverted and abused. The resultant social and economic consequences of these drawbacks are a source of continuing concern.²

*Corresponding author. Tel.: +1 732 690 4960., nyprphd@yahoo.com (C. Santini).

†Current address: 24780 Chieftain Road, Lawrence, KS 66044, USA.

As an alternative to opiates, peripherally-acting agents, of whom NSAIDs are the most familiar examples, have been less useful when pain is in the moderate to severe range.³ Peripheral agents act by altering molecular and physiological events at the site where the pain signal is generated instead of where the signal is received or perceived in the CNS.⁴ In doing so, peripheral agents present a major advantage in that they do not alter consciousness, do not produce other deleterious CNS side effects nor do they interfere with the analgesic actions of centrally-acting agents such as opiates. Despite these advantages, available peripheral agents have not demonstrated efficacy as replacements for centrally acting agents. Currently known peripheral analgesics do not block the initiation of pain signals with the specificity and to the extent required for the improvement in the quality of life of chronic pain patients.

The initial step of pain sensation is the generation of action potential(s) by ion channel mediated depolarization of sensory nerve terminals in skin or deep tissues.⁵ Preventing the generation of these nociceptive signals at their origin by inhibiting the ion channels responsible for the depolarization would provide highly effective analgesia since a pain signal that is not generated is one that requires no blockage further upstream in the CNS. However, there are a multitude of ion channels in nociceptive nerve endings that can respond to algogenic chemicals released from damaged cells. For this reason blocking only one channel does not appear to provide the efficacy necessary for a useful analgesic agent. Alternatively, it may be possible to administer an agent that will temporarily disable the nociceptive nerve endings but only in the localized areas directly implicated in the painful condition, essentially acting as a highly specific, activity dependent long-term analgesic.

TRPV1 is a high-conductance, non-specific cation channel both restricted to and highly expressed in a subpopulation of nociceptive afferents. The receptor is activated by small-molecule ligands, noxious heat (>42 °C) and extracellular protons, contributing to pain sensation under pathological conditions like chronic inflammation (arthritic pain) or chemotherapy-induced and diabetic neuropathies.⁶ Initial enthusiasm to develop small-molecule antagonists of TRPV1 that bind at the capsaicin recognition site as a novel class of analgesics to 'block pain at the source' faded as side effects stemming from less-studied physiological roles of TRPV1 emerged during clinical trials.⁷

As an alternative to antagonists, we have been working on the development of both potent agonists and positive allosteric modulators (PAMs) of TRPV1 as analgesic agents. Both can temporarily incapacitate TRPV1 expressing nerve terminals through calcium overload. Potent agonists like resiniferatoxin (RTX) affect all TRPV1 positive nerve endings, while PAMs act only at nerve terminals with activated TRPV1, in a state-dependent manner.⁸ Local administration of potent TRPV1 agonists or oral administration of TRPV1 PAMs could provide a new class of analgesics and a much sought-after alternative to opioids in pain control. Designing or discovering such agents could be rendered more facile with increased understanding of the structure of the relevant ion channels. The structure of TRPV1 has not yet been solved and, in an effort to acquire understanding of its structure and pharmacology, a screening program was undertaken to identify either agonists or allosteric modulators.

A high-throughput screen of the NIH Small Molecule Repository (SMR) revealed a series of geometrically constrained TRPV1 agonists, possessing structural features reminiscent of capsaicin, with compound MLS002174161 showing highest potency (Fig. 1).⁹ In order to better understand the spatial organization of the TRPV1 agonist pharmacophore responsible for the activity of MLS002174161, a series of related compounds was proposed for synthesis and SAR study. Given the structure, we believed that closely related compounds could be prepared using a method similar to that of Grigg and used later by Kurth, followed by modifications at the nitrogen atom and ester (Scheme 1).¹⁰ In this sequence phenol **1a** was first alkylated with commercially available ethyl trans-4-bromo-2-butenolate to afford **2a** in 49% yield.¹¹ Aldehyde **2a** was next converted to imines **3a** and **3b** through reaction with the methyl or benzyl esters of alanine HCl salt in the presence of Hünig's base and 4 Å molecular sieves. From here, the imines **3a** and **3b** were converted to their corresponding cycloadducts **4a** and **4b** in 55% and 44% yields, respectively. The cycloadducts were obtained as single diastereomers, with the relative configurations shown, as described in earlier reports. The cycloadducts **4** were racemic regardless of whether or not chiral alanine esters were used.¹⁰

Attempts to acylate the secondary nitrogen atom using aromatic acyl chlorides to afford various amides were not successful. We were, however, able to prepare the related hydantoins **6a** and **6b** using methyl ester **4a** by reaction with aryl isocyanates followed by intramolecular ring closure in a manner similar to Kurth's example (Scheme 2).^{10b} This observation led us to conclude that only the most reactive and unhindered electrophiles can react with this particular nitrogen atom. Again, the stereochemistry is implied from the previous reports, although Kurth notes epimerization at the α -position to the methyl ester occurs under the basic conditions employed for ring closure of glycine derivatives. In our alanine derived case, the presence of the additional methyl group prevents epimerization.

After encountering more difficulties in diversifying the α -methyl substituted ester group in **4a** and **4b** a new strategy was employed in which the amide portion was preassembled prior to imine formation (Scheme 3). The resultant α -iminoamides **11** could then be subjected to the 1,3-dipolar cycloaddition conditions to afford the desired amide compounds in a convergent fashion. To the best of our knowledge, there have been few reports of α -iminoamides being used in this type of azo-methine ylide 1,3-dipolar cycloaddition, with most examples appearing as part of a larger series that contain mostly esters.¹² Only one report, published in 2012, focuses exclusively on this class of substrates.¹³ Of all the 1,3-dipolar cycloaddition reactions of α -iminoamides found, we encountered no intramolecular examples.

We first needed to synthesize a suitable α -aminoamide. For reasons related to our previous initial screening study, we wished to couple aniline derivative **8a** to Bocalanine, affording **9a**. This was accomplished (Scheme 3) with EEDQ being crucial to the coupling.¹⁴ Microwave irradiation accelerated the reaction, conveniently providing **9a** in 73% yield. These microwave conditions were adopted for the formation of all subsequent α -aminoamides described in this report. To finish the sequence, TFA salt **10a** was formed by deprotection of **9a**. The conditions shown in Scheme 1 were then used to form α -iminoamide **11a** in 76% yield from **9a**. Effecting the cycloaddition reaction as in Scheme 1

was unsuccessful due to the low solubility of α -iminoamide **11a** in acetonitrile. The reaction was therefore performed in dichloromethane (DCM) using silver fluoride and triethylamine.¹⁵ These conditions afforded the desired product **12a** in 22% yield, but also provided a second product which was, by ¹H NMR spectroscopy, a mixture of two other compounds that showed the absence of the ethyl ester group. LCMS analysis, which showed a single compound, also showed the loss of ethanol from the mass of the cycloadduct **12a**. As a result of variable temperature ¹H NMR spectroscopy coalescence studies and ¹⁵N NMR spectroscopy we assigned the structure of the second product to be imide **13a** (29% yield) as a 2:1 mixture of atropisomers. Using the less basic silver trifluoroacetate in place of silver fluoride also afforded the same products, but gave **13a** in a diminished 13% yield.

To probe the scope and limitations of this method and provide some initial SAR, a series of α -aminoamides and aldehydes was synthesized using the above conditions (Scheme 4).

Deprotection of *N*-Boc-protected α -aminoamides **9** provided their α -aminoamide TFA salts (corresponding to Scheme 3, structure **10**). These TFA salts were combined with aldehydes **2** under the conditions shown in Scheme 3 to provide the desired imines **11** in 58–92% yields in all but one case (Table 1).

Imines **11b**, **c**, **d**, and **e**, derived from **9a** and aldehydes **2b**, **c**, **d** and **e**, underwent AgF promoted cyclization as shown in Scheme 3 to afford mixtures of cycloadducts **12b–e** and their derived imides **13b–e**. Cycloadducts **12b–e** were formed in 19–22% yield and imides **13b–e** in 23–36% yield, respectively (Table 1, entries 1–4).¹⁶ Imine **11f** ($R^1 = H$), obtained from aldehyde **2a** and glycine derived α -aminoamide **9e**, gave cycloadduct **12f** (14% yield) and imide **13f** (28% yield; Table 1, entry 5). We observed, qualitatively, that the conversion of glycine derived **12f** to imide **13f** was more facile than the conversion of alanine derived **12a** to imide **13a**. Cycloadduct **12f** was isolated in pure form by normal phase chromatography. However, during reverse phase HPLC analysis or purification of **12f**, using an aq ammonia (pH 9.4) modified mobile phase, imide **13f** was generated. Imide **13f** did not form under acidic conditions. This apparent ammonia promoted imide formation was not observed for any of the alanine derived compounds.

To shed some light on the structural features that facilitate the conversion of cycloadducts **12** to imides **13**, alanine derived α -aminoamides **9b**, **9c** and **9d** were used to form imines **11g**, **11h** and **11i** from aldehyde **2a**. Imines **11g** and **11h** were synthesized in 83% and 75% yields respectively and subjected to the silver-mediated cyclization conditions (Table 1, entries 6 and 7). **9d** failed to form imine **11i** (Table 1, entry 8).

We initially hypothesized that the electron-withdrawing aryl *ortho*-carboxymethyl substituent facilitated the conversion of cycloadducts **12** to imides **13** solely by lowering the pKa of the anilide proton just enough that some polarization of the N–H bond would occur. The bond polarization would increase the negatively charged character of the nitrogen and lead to imide formation. In keeping with this idea, we were not surprised that **11g** did not undergo this process, giving only cycloadduct **12g** (20% yield; Table 1, entry 6) with no accompanying formation of imide **13g**. We then predicted that the *para*-carboxymethyl substituent of **11h** would exert a similar effect, giving first cycloadduct **12h** and then imide

13h. This did not occur. Aryl *para*-carboxymethyl **11h** gave only cycloadduct **12h** (44% yield; Table 1, entry 7) without spontaneously affording the imide **13h**. This did not support our 'pKa lowering' hypothesis. Another experiment using aryl *ortho*ethyl species **11j** was carried out (Table 1, entry 9). The electronically neutral, but sterically congested, *ortho*-ethyl **11j** also stopped reacting at the initial cycloadduct stage, giving **12j** (28% yield) without formation of imide **13j**. Thus only the electron-withdrawing, sterically congested *ortho*-esters afforded imides. We concluded that both of the preceding factors are needed to convert the cycloadducts **12** to the imides **13**.

Two fully *N*-substituted α -iminoamides **11k** (from α -*N*-Bocaminoamide **9f** and aldehyde **2a**) and **11n** (from α -*N*-Boc-aminoamide **9g** and aldehyde **2d**) were also prepared and subjected to AgF promoted cyclization. Alanine derived imine **11k** failed to afford any cycloadduct or imine products (Table 1, entry 10). Glycine derived imine **11n** afforded cycloadduct **12n** in 42% yield with no imine **13n** formed (Table 1, entry 11). We believe A_{1,3} strain that is present in the formation of the azo-methine intermediate in *Int-11k* prevents the cycloaddition reaction from easily occurring. This strain would not be present in the case of *Int-11n* or when employing a secondary amide such as shown by *Int-11a* (Scheme 5).

Finally, to assess the accuracy of our assignments of relative stereochemistry with respect to the cycloadducts that were obtained using the α -iminoamides cycloadduct **12n**, purified to >99 area% as analyzed by High Resolution LCMS, was crystallized from 0.1 N HCl. The crystallization afforded two crystal forms: a triclinic unit cell as a needle and a monoclinic unit cell as a plate. X-ray crystallographic data for the plate was obtained (deposition #CCDC 972332), showing the product as its monohydrate with the relative stereochemistry we expected based on Kurth's precedent (Fig. 2). The needles were not characterized by X-ray.

The synthesized compounds **4a**, **6a**, **6b**, **12a–h**, **12j**, **12n**, **13a–f** were assayed for TRPV1 agonist activity. The activity of the above compounds that showed agonist properties is shown in Fig. 3. Four compounds, **12a**, **12e**, **12b** and **12d** showed partial agonism.

The structures of all the compounds tested can be classified into three main categories based on the scheme proposed by Walpole (refer to the above color-coded region structure of capsaicin, Fig. 1A).⁸ Compound **4a** falls into the first group. This compound lacks the benzyl group corresponding to region 'A' in Walpole's scheme, resulting in the expected loss of agonist activity. Group 2 consists of compounds displaying the benzyl moiety together with an additional methyl-, carboxymethyl group, or both (compounds **12a**, **12g**, **12e**, **12c**, **12b**, **12h**, **12d**, **12f** and **12n**). In addition, the nitrogen adjacent to the benzyl ring forms an amide bond, showing good correspondence to the 'B' region of capsaicin. The third group consists of compounds where the nitrogen adjacent to the benzyl group is incorporated into either a hydantoin ring or an imide ring and ceases to behave as a hydrogen bond donor (compounds **13a**, **6a**, **6b**, **13e**, **13c**, **13b**, **13d** and **13f**), while also reducing their flexibility.

All TRPV1 agonists identified (**12a**, **12e**, **12b** and **12d**) belong to the second group. Their structure relative to capsaicin and their lower potency align well with observations made by

Walpole: (1) removing the single sp^3 carbon 'spacer' separating the benzyl group from the amide group results in a ten-fold reduction of potency {**3a–b**, Table 1, Walpole region 'B' 1993} (2) eliminating the H-bond donor nitrogen from the amide bond also takes a significant toll on potency {**3a** vs **20**, Table 1, Walpole region 'B' 1993} (3) additional groups on the benzyl 'A' region are far from the optimal 4-Hydroxy 3-methoxy groups found in capsaicin {**2b**, Table 1, Walpole region 'A', 1993}.

Conclusions

We have identified a novel, spatially constrained, TRPV1 agonist and four *seco* analogs with partial TRPV1 agonist activity. Using the alignment of the active analogs, capsaicin and the fully rigid agonist MLS002174161, we propose a three-dimensional TRPV1 agonist pharmacophore comprised of aromatic, hydrophobic, hydrogen-bond donor and acceptor moieties, complete with directional information about the expected locations of donor and acceptor partners. We expect that, following further validation, the above proposed pharmacophore model will facilitate the development of potent TRPV1 agonists with potential use in the treatment of localized, chronic pain.

Acknowledgments

We acknowledge Mr. Patrick Porubsky, KU-CMLD Purification Chemist and Compound Curator. Financial support for the KUCMLD was provided under NIGMS Grant #5P50GM069663 (Prof. Jeff Aubé, PI). Support for the KU-NMR Center (JTD) was provided under Grant #NIH 1S10RR024664-01. Support for the KU-X-Ray facility (VWD) was provided under NSF-MRI Grant CHE-0923449. Support for the HTS screen was provided by NIMH Grant # 1 R03 MH089480-01 (M. Iadarola); research was also supported by the Division of Intramural Research, NIDCR, NIH and the Department of Perioperative Medicine, Clinical Center, NIH. The funding sources did not participate in the design of the work described in this report.

References and notes

1. For a comprehensive review on opiates and related material, see: McCurdy CR, Prisinzano TE. Opioid receptor ligands. Burger's Medicinal Chemistry, Drug Discovery and Development (7). Abraham DJ, Rotella DP. John Wiley & Sons New York 2010; 8:569.
2. (a) McCabe SE, West BT, Boyd CJJ. *Adolesc Health*. 2013; 52:480. (b) McNeely J, Gourevitch MN, Paone D, Shah S, Wright S, Heller D. *Biomed Central Public Health*. 2012; 12:443. [PubMed: 22713674]
3. For a review on COX-2 inhibitors, see: Bell RL, Harris RR, Stewart AO. COX-2 Inhibitors and Leukotriene Modulators. Burger's Medicinal Chemistry, Drug Discovery and Development. Abraham DJ, Rotella DP. John Wiley & Sons New York 2003; 5:193.
4. For a comprehensive reference on peripheral pain receptor targets, see: Peripheral Receptor Targets for Analgesia: Novel Approaches to Pain Management. Cairns BE. John Wiley & Sons Hoboken 2009
5. For a review on the pain pathway, see: Millan MJ. *Prog Neurobiol*. 1999; 57:1. [PubMed: 9987804]
6. For selected references on TRPV1, see: Trevisani M, Szallasi A. Vanilloid, (TRPV1) and Other Transient Receptor Potential Channels. Peripheral Receptor Targets for Analgesia: Novel Approaches to Pain Management. Cairns BE. John Wiley & Sons Inc Hoboken, NJ 2009:175. Caterina MJ, Schumacher MA, Tominaga M, Rosen TA, Levine JD, Julius D. *Nature*. 1997; 389:816. [PubMed: 9349813] Caterina MJ, Julius D. *Annu Rev Neurosci*. 2001; 24:487. [PubMed: 11283319] Kárai L, Russell JT, Iadarola MJ, Oláh Z. *J Biol Chem*. 2004; 279:16377. [PubMed: 14963041] Kaszas K, Keller JM, Coddou C, Mishra SK, Hoon MA, Stojilkovic S, Jacobson KA, Iadarola MJ. *J Pharmacol Exp Ther*. 2012; 340:152. [PubMed: 22005042]

7. For selected historical accounts and clinical trials on TRPV1 antagonists, see: Szallasi A, Cortright DN, Blum CA, Eid SR. *Nat Rev Drug Discovery*. 2007; 6:357. [PubMed: 17464295] Gavva NR, Treanor JJS, Garami A, Fang L, Surapaneni S, Akrami A, Alvarez F, Bak A, Darling M, Gore A, Jang GR, Kessler JP, Ni L, Norman MH, Palluconi G, Rose MJ, Salfi M, Tan E, Romanovsky AA, Banfield C, Davar G. *Pain*. 2008; 136:202. [PubMed: 18337008] Gunthorpe MJ, Chizh BA. *Drug Discovery Today*. 2009; 14:56. [PubMed: 19063991] Knotkova H, Pappagallo M, Szallasi A. *Clin J Pain*. 2008; 24:142. [PubMed: 18209521] Gunthorpe MJ, Szallasi A. *Curr Pharm Des*. 2008; 14:32. [PubMed: 18220816] Krarup AL, Ny L, Åstrand M, Bajor A, Hvid-Jensen F, Hansen MB, Simrén M, Funch-Jensen P, Drewes AM. *Aliment Pharmacol Ther*. 2011; 33:1113. [PubMed: 21410733] Khairatkar-Joshi N, Szallasi A. *Mol Med*. 2009; 15:14. Kym PR, Kort ME, Hutchins CW. *Biochem Pharmacol*. 2009; 78:211. [PubMed: 19481638]
8. For selected references on RTX, see: Szallasi A, Blumberg PM. *Neuroscience*. 1989; 30:515. [PubMed: 2747924] Szallasi A, Blumberg PM. *Life Sci*. 1990; 47:1399. [PubMed: 2174484] Wender PA, Jesudason CD, Nakahira H, Tamura N, Tebbe AL, Ueno Y. *J Am Chem Soc*. 1997; 119:12976. Kissin I, Szallasi A. *Curr Top Med Chem*. 2011; 11:2159. [PubMed: 21671878] Bates BD, Mitchell K, Keller JM, Chan CC, Swaim WD, Yaskovich R, Mannes AJ, Iadarola M. *J Pain*. 2010; 149:522. Mitchell K, Bates BD, Keller JM, Lopez M, Scholl L, Navarro J, Madian N, Haspel G, Nemenov MI, Iadarola MJ. *Mol Pain*. 2010; 6:94. [PubMed: 21167052] Iadarola MJ, Mannes AJ. *Curr Top Med Chem*. 2011; 11:2171. [PubMed: 21671877]
9. For reports on capsaicin SAR, see: Walpole CSJ, Wrigglesworth R, Bevan S, Campbell EA, Dray A, James IF, Perkins MN, Reid DJ, Winter J. *J Med Chem*. 1993; 36:2362. [PubMed: 8360881] Walpole CSJ, Wrigglesworth R, Bevan S, Campbell EA, Dray A, James IF, Masdin KJ, Perkins MN, Winter J. *J Med Chem*. 1993; 36:2373. [PubMed: 8360882] Walpole CSJ, Wrigglesworth R, Bevan S, Campbell EA, Dray A, James IF, Masdin KJ, Perkins MN, Winter J. *J Med Chem*. 1993; 36:2381. [PubMed: 8360883]
10. (a) Barr DA, Grigg R, Gunaratne HQN, Kemp J, McMeekin P, Sridharan V. *Tetrahedron*. 1988; 44:557. (b) Gong YD, Najdi S, Olmstead MM, Kurth MJ. *J Org Chem*. 1998; 63:3081.
11. Moore JL, Silvestri AP, Read de Alaniz J, DiRocco DA, Rovis T. *Org Lett*. 2011; 13:1742. [PubMed: 21355598]
12. (a) Dondas HA, Grigg R, Kilner C. *Tetrahedron*. 2003; 59:8481. (b) Dondas HA, Soenmez S. *Heterocycl Commun*. 2003; 9:23. (c) Wu SH, Sun WQ, Zhang DW, Shu LH, Wu HM, Xu JF, Lao XF. *J Chem Soc, Perkin Trans*. 1998; 1:1733. (d) Galley G, Liebscher J, Paetzel M. *J Org Chem*. 1995; 60:5005. (e) Grigg R, Donegan G, Gunaratne HQN, Kennedy DA, Malone JF, Sridharan V, Thianpatanagul S. *Tetrahedron*. 1989; 45:1723. (f) Grigg R, McMeekin P, Sridharan V. *Tetrahedron*. 1995; 51:13347. (g) Grigg R, Montgomery J, Somasunderam A. *Tetrahedron*. 1992; 48:10431. (h) Grigg R, Thianpatanagul S, Kemp J. *Tetrahedron*. 1988; 44:7283. (i) Tsuge O, Kanemasa S, Yoshioka M. *J Org Chem*. 1988; 53:1384.
13. González-Esguevillas M, Adrio J, Carretero JC. *Chem Commun*. 2012; 48:2149.
14. Corbo F, Franchini C, Lentini G, Muraglia M, Ghelardini C, Matucci R, Galeotti N, Vivoli E, Tortorella V. *J Med Chem*. 2007; 50:1907. [PubMed: 17373780]
15. Ding, Q.; Jiang, N.; Liu, J-J.; Ross, TM.; Zhang, J.; Zhang, Z. *PCT Int Appl*. WO 2010031713 A1 20100325. 2010.
16. *Representative procedure for formation of imine 11c, and adducts 12c and 13c*: To a solution of the TFA salt of 9a (0.169 g, 0.482 mmol) in dichloromethane (3.40 mL) was added *N,N*-diisopropylethylamine (0.09 mL, 0.506 mmol). The reaction mixture was stirred for 15 min then powdered 4 Å mol sieves (0.50 g) followed by a solution of aldehyde 1b (0.127 g, 0.482 mmol) in DCM (1 mL). The reaction mixture was stirred for 18 h overnight and then diluted with DCM and washed with water (×2) and brine (×1). The organic layer was dried over MgSO₄, filtered and concentrated under vacuum to give the product 11b (0.179 g, 77%) as a yellow oil that was used in the next step without further purification. To a solution of imine 11b (0.179 g, 0.371 mmol) in DCM (4.40 mL) was added triethylamine (0.16 mL, 1.11 mmol) and silver fluoride (0.235 g, 1.85 mmol). The reaction vessel was wrapped in foil and stirred in the dark for 18 h. The reaction was quenched with ammonium chloride (2 mL) and the mixture filtered through a phase separator. The remaining aqueous layer was extracted three times through the phase separator with DCM and the combined organic layers were dried over MgSO₄, filtered, and concentrated under vacuum. The residue was purified via silica gel column chromatography (10–50% ethyl acetate in hexanes) to

give 12b (0.039 g, 22%) and 13b (0.059 g, 36%) as white, amorphous solids. 12b: ^1H NMR (500 MHz, CDCl_3) δ 12.38 (s, 1H), 8.61 (s, 1H), 7.88 (d, $J = 8.2$ Hz, 1H), 6.89 (m, 1H), 6.85 (d, $J = 9.0$ Hz, 1H), 6.78 (dd, $J = 9.0, 3.0$ Hz, 1H), 6.44 (d, $J = 2.9$ Hz, 1H), 4.95 (dd, $J = 11.1, 2.2$ Hz, 1H), 4.68 (d, $J = 2.9$ Hz, 1H), 4.16 (q, $J = 7.1$ Hz, 2H), 4.16 (m, 1H), 3.77 (s, 3H), 3.71 (s, 3H), 2.55–2.46 (m, 3H), 2.44 (s, 3H), 2.40 (s, 3H), 1.26 (t, $J = 7.1$ Hz, 3H); ^{13}C NMR (125 MHz, CDCl_3) δ 172.1, 167.5, 163.3, 161.0, 153.5, 148.1, 145.2, 140.0, 131.0, 123.7, 121.0, 120.5, 117.7, 115.2, 114.4, 114.0, 66.0, 60.7, 59.2, 55.7, 51.8, 35.3, 33.9, 22.0, 14.2, 13.1; IR: 3234, 2953, 1731, 1694 cm^{-1} ; HRMS (ESI) m/z calculated for $(\text{M}+\text{H})^+$ ($\text{C}_{26}\text{H}_{31}\text{N}_2\text{O}_7$) $^+$ 483.2131, found 483.2155; 13b: HRMS (ESI) m/z calculated for $(\text{M}+\text{H})^+$ ($\text{C}_{24}\text{H}_{25}\text{N}_2\text{O}_6$) $^+$ 437.1713, found 437.1718.

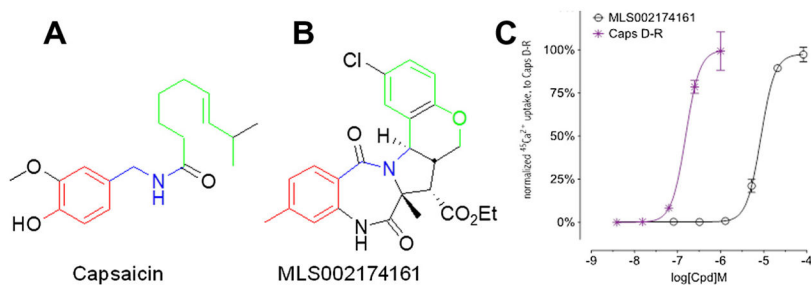


Figure 1. High-throughput screen identified a constrained TRPV1 agonist. (A) Structure of capsaicin, archetypical vanilloid TRPV1 agonist. Color coding highlights structural subdivision according to Walpole, **1993** (red = region A, blue = region B, green = region C) (B) MLS002174161, a fully constrained rigid TRPV1 agonist with proposed alignment of capsaicin (C) MLS002174161 is a full agonist of TRPV1 with reduced potency compared to capsaicin. This reduction of potency is expected due to the rigidity of the ligand.

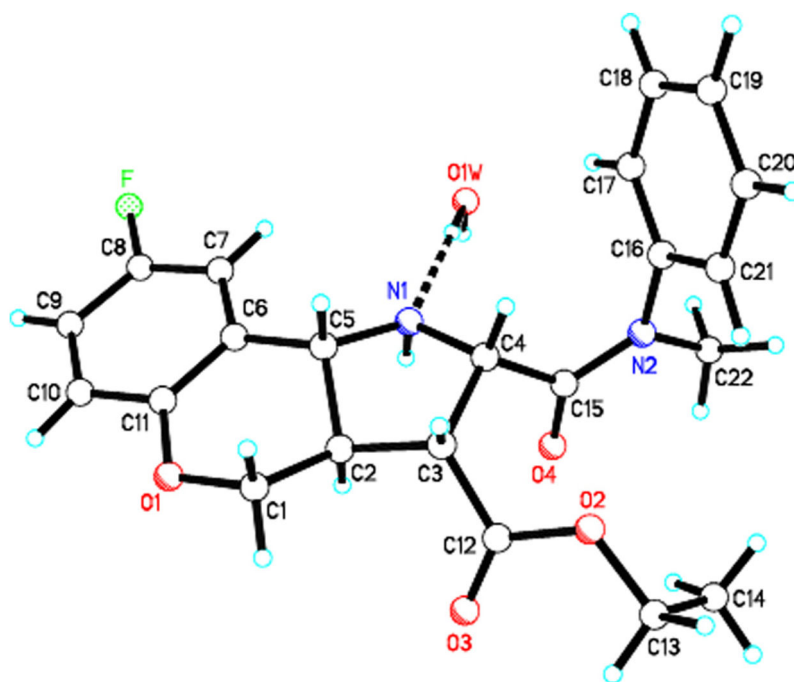


Figure 2.
X-ray crystal structure of **12n** as its monohydrate.

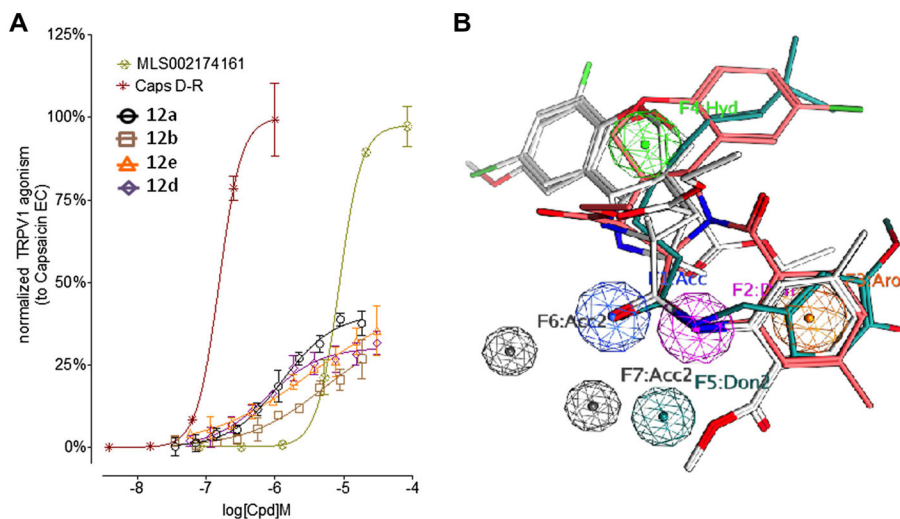
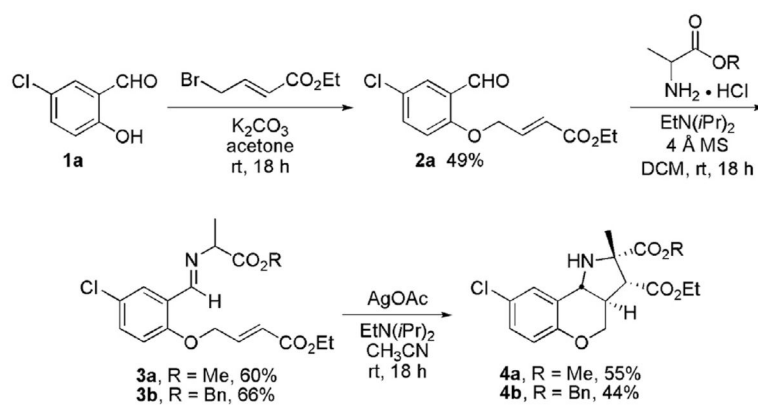
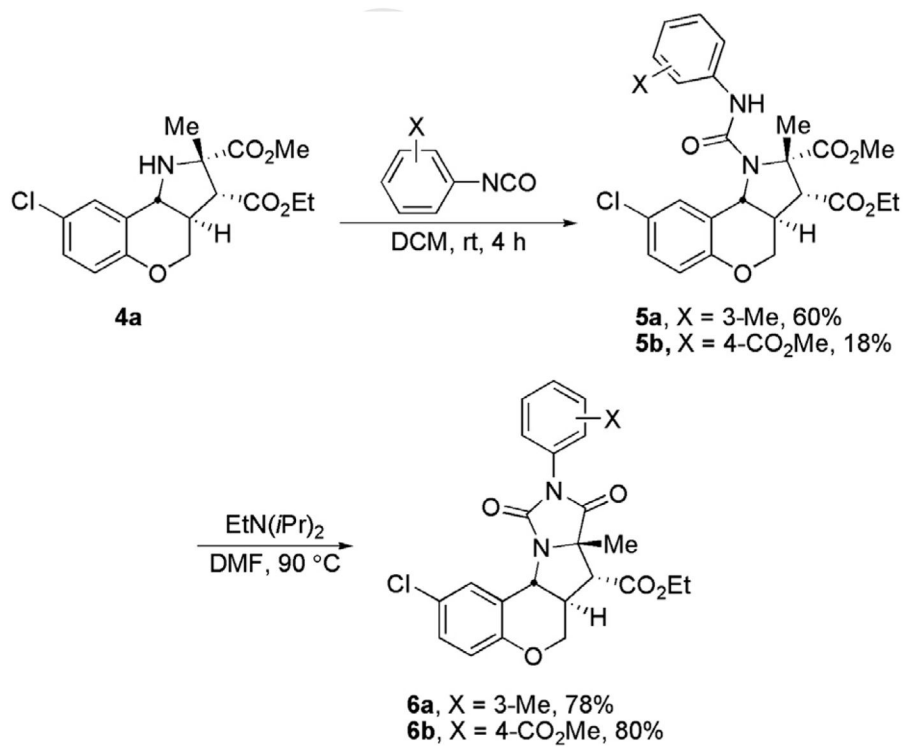


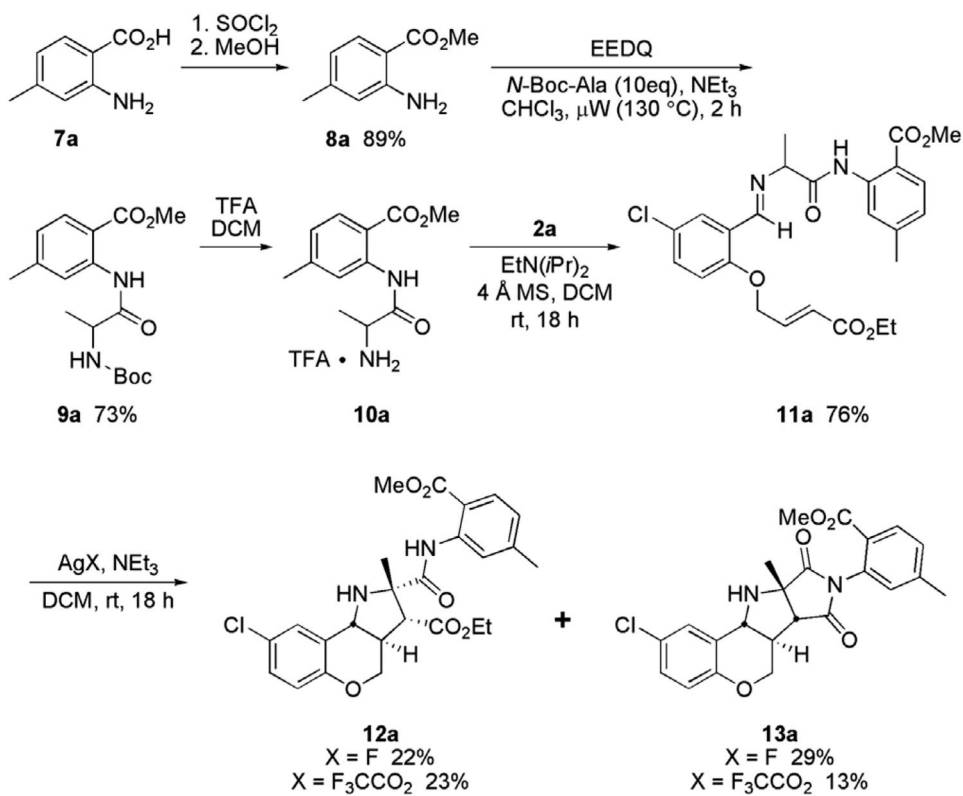
Figure 3. Biological activity of synthesized compounds on TRPV1 using a $^{45}\text{Ca}^{2+}$ uptake assay. (A) Four out of the eighteen compounds exhibited TRPV1 agonist activity. Compounds **12a**, **12e**, **12b** and **12d** all behave as partial TRPV1 agonists with **12e** showing the lowest potency and efficacy. (B) Proposed alignment of capsaicin (cyan), MLS002174161 (salmon) and the four partial agonists (light grey). The proposed alignment shows good overlap of an **Aromatic center** (orange) and a **Hydrophobic region** (green) between all compounds. They also exhibit closely localized hydrogen-bond **Donor** (pink) and **Acceptor** (blue) groups and similarly tight grouping of hydrogen-bond donor and acceptor projections (Don2 (dark cyan) and Acc2 (grey), respectively).



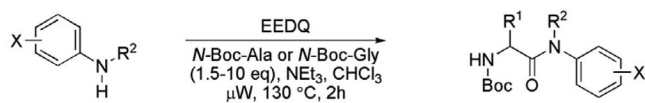
Scheme 1.
Synthesis of the initially proposed ester scaffolds.



Scheme 2.
Synthesis of hydantoin **6**.

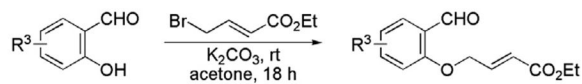


Scheme 3.
 Synthetic sequence for formation of **12a** and **13a**.



- 8a** R² = H, X = 2-CO₂Me, 5-Me
8b R² = H, X = 3-Me
8c R² = H, X = 4-CO₂Me
8d R² = H, X = 2,6-diMe
8e R² = Me, X = H
8f R² = H, X = 2-Et

- 9a** R¹ = Me, R² = H, X = 2-CO₂Me, 5-Me; 73%
9b R¹ = Me, R² = H, X = 3-Me; 79%
9c R¹ = Me, R² = H, X = 4-CO₂Me; 53%
9d R¹ = Me, R² = H, X = 2,6-diMe; 94%
9e R¹ = H, R² = H, X = 2-CO₂Me, 5-Me; 70%
9f R¹ = Me, R² = Me, X = H; 82%
9g R¹ = H, R² = Me, X = H; 85%
9h R¹ = Me, R² = H, X = 2-Et; 88%

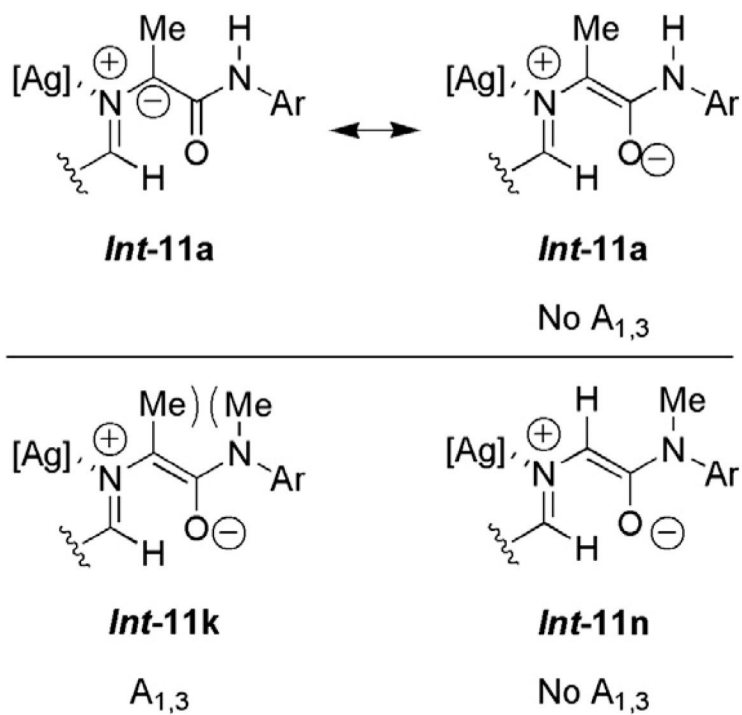


- 1a** R³ = 5-Cl
1b R³ = 5-OMe
1c R³ = 4-OMe
1d R³ = 5-F
1e R³ = 3-F

- 2a** R³ = 5-Cl; 49%
2b R³ = 5-OMe; 58%
2c R³ = 4-OMe; 40%
2d R³ = 5-F; 50%
2e R³ = 3-F; 56%

Scheme 4.

Synthesis α -aminoamides and aldehydes.



Scheme 5.
Proposed $A_{1,3}$ Strain of 1,3-dipole ***Int-11k*** vs. ***Int-11a*** and ***Int-11n***.

Table 1

Synthesis of imines **11**, cycloadducts **12** and imides **13** (N/A = not applicable)

Entry	Ar	R ¹	R ²	R ³	Imine 11 , yield	Cycloadduct 12 , yield	Imide 13 , yield
1		Me	H	5-OMe	11b , 77%	12b , 22%	13b , 36%
2	"	Me	H	4-OMe	11c , 91%	12c , 21%	13c , 23%
3	"	Me	H	5-F	11d , 82%	12d , 19%	13d , 30%
4	"	Me	H	3-F	11e , 74%	12e , 19%	13e , 26%
5	"	H	H	5-Cl	11f , 92%	12f , 14%	13f , 28%
6 ^a		Me	H	5-Cl	11g , 83%	12g , 20%	Not observed
7		Me	H	5-Cl	11h , 75%	12h , 44%	Not observed
8		Me	H	5-Cl	11i , Not observed	N/A	N/A

Entry	Ar	R ¹	R ²	R ³	Imine 11, yield	Cycloadduct 12, yield	Imide 13, yield
9 ^b		Me	H	5-Cl	11j, 90%	12j, 28%	Not observed
10	Ph	Me	Me	5-Cl	11k, 58%	Not observed	N/A
11	Ph	H	Me	5-F	11n, 79%	12n, 42%	Not observed

^a Reaction performed with AgCO₂CF₃.

^b 36 h reaction time.